Heliyon 11 (2025) e42894

Contents lists available at ScienceDirect

Heliyon

journal homepage: www.cell.com/heliyon

Research article

Proliferation and migration inhibition of adenoid cystic carcinoma cells through autophagy suppression via GLUT1 knockdown☆

Kan Liu [a], Jinlong Zhu [b], Yangyang Bao [b], Jin Fang [a,*], Shuihong Zhou [b], Jun Fan [c]

[a] Department of Otolaryngology, Zhejiang Sian International Hospital of Jiaxing City, Jiaxing City, Zhejiang Province, China
[b] Department of Otolaryngology, The First Affiliated Hospital, College of Medicine, Zhejiang University, Hangzhou, Zhejiang, China
[c] State Key Laboratory for Diagnosis and Treatment of Infectious Diseases, The First Affiliated Hospital, College of Medicine, Zhejiang University, Hangzhou, Zhejiang, China

ARTICLE INFO

Keywords:
Adenoid cystic carcinoma
Hypoxia
Glucose transporter-1
Autophagy
Chloroquine

ABSTRACT

Multiple studies have demonstrated a significant association between glucose transporter-1 (GLUT1) and the development and recurrence of adenoid cystic carcinoma (ACC). In this study, we investigated the impact of GLUT1 knockdown on adenoid cystic carcinoma. Our findings revealed that hypoxic conditions promoted the progression and autophagy of SACC83 and SACC-LM cell lines, an effect that was mitigated by GLUT1 knockdown. In vivo experiments showed that the combination of lentivirus-delivered GLUT1 shRNA and autophagy inhibitor chloroquine (CQ) produced the most substantial reduction in tumor volume, weight, Ki67 expression, and autophagy in tumor tissues. In conclusion, hypoxia facilitates ACC progression by upregulating GLUT1 expression. The suppression of GLUT1 expression and autophagy effectively inhibited ACC cell proliferation both *in vitro* and *in vivo*.

1. Introduction

Adenoid cystic carcinoma (ACC) is a rare malignancy that originates from major and minor salivary glands, lacrimal glands, paranasal sinuses, and other regions of the head and neck, as well as the mammary glands, skin, and genitalia[1–3]. Because of its hidden location, the early symptoms of ACC in the head and neck are often atypical [1,4]. Early-stage ACC frequently exhibits nerve invasion, local recurrence, and distant metastasis, leading to a poor prognosis [1,4]. Currently, the primary treatment for ACC is surgical intervention, with or without radiotherapy. Despite new targeted therapies, the 5-year survival rate has not significantly improved [1,4]. This poor prognosis is result of insufficient information concerning ACC etiology and pathogenesis. Thus, investigations of ACC etiology and pathogenesis are particularly important.

Similar to most malignant tumors, the physiological environment of ACC is characterized by local hypoxia that results from an insufficient oxygen supply[5–8]. Under hypoxic conditions, cancer cells undergo metabolic adaptation through the Warburg effect, which involves glycolysis and a significant increase in glucose uptake[9–13]. Glucose transporter-1 (GLUT1) is important for glucose uptake and transportation in cancer cells[11–14]. Multiple studies have demonstrated that high GLUT1 expression in malignant tumors is associated with bio-behavioral factors and treatment resistance[13,15–21]. Our previous study showed that GLUT1 is involved

☆ The English in this document has been checked by at least two professional editors, both native speakers of English. For a certificate, please see: http://www.textcheck.com/certificate/w7Fvuu.

* Corresponding author.
E-mail address: 2834632323@qq.com (J. Fang).

https://doi.org/10.1016/j.heliyon.2025.e42894
Received 18 September 2024; Received in revised form 19 February 2025; Accepted 20 February 2025
Available online 20 February 2025

in the development and recurrence of ACC [22]. Another study revealed that inhibition of GLUT1 expression could suppress the growth of ACC cells [23]. However, the underlying mechanism by which GLUT1 affects the development of ACC remains unclear.

Recent studies have demonstrated that autophagy is involved in tumorigenesis, tumor development, and chemoradiotherapy resistance[19,24–26]. Investigations of autophagy in patients with ACC have revealed that autophagy-related genes are involved in ACC tumorigenesis and can serve as prognostic factors[6,7,27–31]. Moreover, autophagy inhibition can improve ACC chemosensitivity [30]. GLUT1 promotes the growth and migration of cancer cells through autophagy in various solid tumors [26,32]. Our previous study demonstrated that $CD133^+$ laryngeal cancer cells achieve increased proliferation and migration under hypoxic and low glucose states by upregulating GLUT1 expression and enhancing autophagy [19]. Therefore, GLUT1 knockdown or autophagy inhibition can reduce the proliferation and migration of $CD133^+$ laryngeal cancer stem cells [19]. Additionally, GLUT1 inhibition can improve radiosensitivity in laryngeal carcinoma by regulating autophagy [26]. To our knowledge, no study has investigated the role of GLUT1 in ACC.

In this study, we investigated the association between GLUT1 expression and ACC development in a hypoxic microenvironment, then examined whether the relationship is autophagy-dependent. Additionally, we explored whether targeted inhibition of GLUT1 and autophagy could suppress ACC development *in vitro* and *in vivo*.

2. Materials and methods

2.1. Cell culture

The ACC cell lines SACC83 (MZ-0978) and SACC-LM (MZ-0979) were obtained from Mingzhou Biotechnology Co., Ltd. (Ningbo, China). SACC83 was derived from the sublingual gland of a patient with adenoid cystic carcinoma (ACC), while SACC-LM was established from mouse tissue following tail vein injection of SACC83 cells with a high potential for lung metastasis [33]. The cells were cultured in RPMI-1640 medium (Gibco, Rockville, MD, USA) supplemented with 10 % heat-inactivated fetal bovine serum (HyClone, Logan, UT, USA), 100 U/mL penicillin, and 100 μg/mL streptomycin. For experiments, cells were maintained under normoxic (5 % CO_2, 21 % O_2, 74 % N_2) or hypoxic (5 % CO_2, 1 % O_2, 94 % N_2) conditions in a Binder CB-150 dual-gas incubator equipped with CO_2 and O_2 probes [34].

2.2. siRNA transfection

Logarithmic growth-stage cells (5×10^4 per well) were seeded in a 24-well cell culture plate and cultured overnight at 37 °C with 5 % CO_2. An siRNA solution (20 μmol; Sangon Biotech, Shanghai, China) was diluted with 100 μL of serum-free Opti-MEM and incubated for 5 min at room temperature. Then, 3 μL of Lipofectamine™ 2000 (11668019; Invitrogen, Carlsbad, CA, USA) were diluted in 100 μL of Opti-MEM and incubated for 5 min at room temperature. The Lipofectamine™ 2000 and siRNA were mixed; 200-μL aliquots of the mixed solution were added to each well. The cells were then cultured at 37 °C with 5 % CO_2. After 6 h, the mixed solution was aspirated and replaced with 1640-medium. The GLUT1 siRNA sequences were as follows: sense, 5′-CUGUGGGCCUUUUCGUUAATT-3′; antisense, 5′-UUAACGAAAAGGCCCACAGAG-3′. The negative control siRNA sequences were as follows: sense, 5′-UUCUCCGAACGUGUCACGUTT-3′; antisense 5′-ACGUGACACGUUCGGAGAATT-3′.

2.3. Cell Counting Kit-8 assay

Each well of a 96-well plate was seeded with 5×10^4 cells in a volume of 100 μL, then incubated at 37 °C with 5 % CO_2. After transfection with negative control (NC) or GLUT1 siRNA, the cells were treated with or without the autophagy inhibitor chloroquine (CQ; C843545; Macklin, Shanghai, China) under normoxia or hypoxia. Subsequently, 10 μL of Cell Counting Kit-8 (HY-K0301; MedChemExpress, Shanghai, China) solution were added to each well, and the cells were incubated for 2 h. The absorption of the supernatant was measured at 450 nm using a Microplate Reader (Beijing Pulang New Technology Co., Ltd., Beijing, China).

2.4. Clonogenic assay

Single cells were obtained by digestion of differently treated cells using trypsin, then resuspended in culture media. Each suspension was diluted and evenly seeded in a 6-well plate, then incubated at 37 °C with 5 % CO_2 for 2 weeks. When colonies became visible, the supernatant was removed, and the cells were fixed with ice-cold ethanol for 1 h. After the fixing solution had been discarded, the cells were stained with crystal violet for 30 min and photographed.

2.5. Flow cytometry

Cells were subjected to different treatments, washed twice with phosphate-buffered saline (PBS), and centrifuged for 5 min. Next, they were resuspended in 500 μL of binding buffer, then mixed with 5 μL of AnnexinV-FITC and 5 μL of propidium iodide for 10 min in the dark at room temperature, in accordance with the instructions of the AnnexinV-FITC/PI Apoptosis Detection Kit (KGA108; KeyGen BioTech, Nanjing, China). The proportions of non-apoptotic and apoptotic cells were determined in triplicate using flow cytometry with ModFit LT software (Becton Dickinson Biosciences, CA, USA).

2.6. Transwell assay

siRNA-transfected cells were collected by centrifugation at 1000 rpm for 5 min, washed with PBS, and resuspended in serum-free 1640-medium at a density of 3×10^5 cells/mL. Fetal bovine serum (700 μL) was added to each well of a 24-well plate; upper Transwell chambers (3413; Corning-Costar, Corning, NY, USA) were then placed within the plate. Each upper Transwell chamber was seeded with a 200-μL aliquot of cell suspension, with or without Matrigel. The cells were incubated at 37 °C with 5 % CO_2 for 24 h. After incubation, each Transwell chamber was removed, washed with PBS, and fixed in 70 % ice-cold ethanol solution for 1 h. Subsequently, the cells were stained with 0.5 % crystal violet for 20 min. Finally, unmigrated cells were removed from upper Transwell chambers using cotton swabs; the remaining cells were observed and photographed under a microscope.

2.7. Western blotting

Cells and tissue were lysed using cell lysis buffer (P0013B, Beyotime Biotechnology, Shanghai, China) and proteins were extracted from the supernatant. Protein concentrations were determined using the BCA Assay kit (P0012S, Beyotime Biotechnology). The protein samples were mixed with 5 × loading buffer, boiled in a metal bath for 5–10 min, cooled, and centrifuged. Proteins were separated by sodium dodecyl sulfate–polyacrylamide gel electrophoresis and transferred to a polyvinylidene difluoride membrane (Millipore, Billerica, MA, USA). Primary antibodies against GLUT1 (1:1000; AF0173; Affinity, Wuhan, China), LC3 (1:1000; AF5402; Affinity), p62 (1:1000; Ab109012; Abcam, Hangzhou, China), or β-actin (1:1000; BM0627; Boster, Wuhan, China) were added and the membranes were incubated overnight at 4 °C. Secondary antibodies—goat anti-rabbit IgG (H + L) horseradish peroxidase (HRP) (1:5000; S0001; Affinity) or goat anti-mouse IgG (H + L) HRP (1:5000; BA1051; Boster)—were added and the membranes were incubated for 1 h at 37 °C. The enhanced chemiluminescence reagent and stable peroxidase solution (WP20005; Invitrogen) were mixed in a 1:1 ratio; the resultant working solution was added to the piezoelectric polyvinylidene fluoride film. After reaction for a few minutes, excess substrate solution was removed by filter paper until fluorescence bands were visible; subsequently, the plastic film was covered. X-ray film exposure was conducted; the film was then placed into developing and fixing solutions. The results of western blotting were analyzed using ImageJ software (National Institutes of Health, Bethesda, MD, USA).

2.8. Phalloidin and GLUT1 detection

Sections were fixed with 4 % paraformaldehyde for 15 min, then immersed three times in PBS. Normal goat serum was added to the sections at room temperature for 30 min, followed by overnight incubation at 4 °C with diluted primary antibody against GLUT1 (1:200; AB115730; Abcam). Sections were then washed with PBS and incubated with diluted fluorescent secondary antibody (sheep anti-rabbit Cy3; S0011; Affinity) in a humid incubation chamber at 37 °C for 1 h. Next, the sections were washed with PBS three times, incubated with 5 μg/mL of diluted fluorescein-labeled phalloidin (P5282; Sigma, Shanghai, China) at 37 °C for 1 h, and washed with PBS three more times. DAPI (Sigma-Aldrich, St. Louis, MO, USA) was added and sections were incubated in the dark for 5 min to stain nuclei. Subsequently, sections were washed with PBS to remove excess DAPI, then sealed with a sealing liquid containing an anti-fluorescence quench agent. Finally, images were collected via laser confocal microscopy.

2.9. GFP-LC3 detection

After cells had been treated, the original culture medium was removed, and 1.2 mL of fresh culture medium were added to each well. Then, 10 μL of AD-GFp-LC3 viral fluid (C3006; Beyotime Biotechnology) were added. After 24 h of incubation, virus-containing culture medium was removed and 2 mL of fresh complete culture medium were added to each well. DAPI was added and cells were incubated in the dark for 5 min, then washed with PBS plus Tween four times for 5 min each. The distribution of GFP-LC3 aggregates was observed using a fluorescence microscope (BX53; Olympus, Tokyo, Japan).

2.10. Determination of glucose uptake

Glucose uptake was evaluated using fluorescent glucose 2-NBDG (N13195; Thermo Fisher Scientific, Waltham, MA, USA). Cells were cultured in a 96-well plate in 1640-medium without sources of glucose or carbon. After transfection with GLUT1 siRNA or NC siRNA, the cells were cultured under normoxic or hypoxic conditions. Fluorescence intensity (y) was measured on a microplate reader at an excitation wavelength of 465 nm and an emission wavelength of 540 nm to determine glucose uptake.

2.11. Detection of lactic acid

Lactic acid content was measured using a lactic acid assay kit (BC2235; Solarbio, Beijing, China). Measuring, control, standard, and blank tubes were prepared. First, 10 μL of sample, 10 μL of standard, and 10 μL of distilled water were sequentially added to the measuring and control tubes. Then, 40 μL of reagent 1, 10 μL of reagent 2, 20 μL of reagent 4, 6 μL of reagent 5, and 60 μL of reagent 3 were sequentially added to all tubes. The tubes were centrifuged at 10000 rpm for 10 min, and the supernatant was removed. Finally, 20 μL of ethanol were added to the precipitate, and the optical density of each well was measured at a wavelength of 570 nm after dissolution.

2.12. Animal experiments

All animal experiments were conducted in accordance with the guidelines for the Care and Use of Laboratory Animals and were approved by the Animal Ethics Review Committees of the First Affiliated Hospital, College of Medicine, Zhejiang University (approval no. 2021-009). All experiments were performed in accordance with relevant guidelines and regulations. And all methods are reported in accordance with ARRIVE guidelines.

2.13. Mouse model of ACC

Female BALB/c nude mice, aged 6–8 weeks and weighing 15–19 g, were obtained from Suzhou Huachuang Xinuo Pharmaceutical Technology Co., Ltd. (License No. SCXK(Su)2020-0009, Suzhou, China). Each mouse was then subcutaneously inoculated with 0.2 mL of SACC or SACC-LM cells (2×10^7 cells/ml) in the right flank. All tumors were allowed to grow for approximately 1 week until they reached a volume of 100–150 mm^3. The xenograft mice were subsequently assigned to one of four groups based on their ACC cells: lentivirus NC shRNA, lentivirus GLUT1 shRNA (VB900062-0405hyc; GLUT1 shRNA: TTGCAGGCTTCTCCAACTGGACCTCAAATTT-CATTGTGGGC; VectorBuilder, Guangzhou, China), lentivirus NC shRNA + CQ, and lentivirus GLUT1 shRNA + CQ. Lentivirus (2×10^6 IU/mouse) was administered intratumorally, whereas CQ (C843545; Macklin, 60 mg/kg twice daily) was injected intraperitoneally.

2.14. Tumor volume and body weight of mice measurement

After cell injection, the tumor volumes and mouse body weights were evaluated at 3-day intervals. Tumor volumes were determined using the following formula: $V = 1/2 \times a^2 \times b$, where a is the short axis and b is the long axis. Mice were euthanized via pentobarbital anesthesia at approximately 4 weeks after injection or when their tumor volume reached 1500 mm^3. The tumors were subsequently excised, weighed, and photographed.

2.15. Hematoxylin-eosin staining

Paraffin sections were sequentially immersed in xylene I (20 min), xylene II (20 min), xylene III (20 min), anhydrous ethanol I (5 min), anhydrous ethanol II (5 min), 95 % alcohol (5 min), 90 % alcohol (5 min), 80 % alcohol (5 min), and 70 % alcohol (5 min). The sections were then soaked in distilled water for 5 min. Subsequently, they were stained with Mayer's hematoxylin (Invitrogen) for 5 min and rinsed in water until the color turned blue. The sections were stained with 1 % water-soluble eosin dye solution (BP-DL010; Sbjbio, Nanjing, China) for 5 min and rinsed in water for 30 s. After sections had been washed with 95 % alcohol (30 s), 90 % alcohol (1 min), anhydrous ethanol I (5 min), anhydrous ethanol II (5 min), xylene I (5 min), and xylene II (5 min), they were air-dried, sealed with neutral gum, and visualized under a light microscope.

2.16. TUNEL staining

Apoptosis was evaluated using a cell apoptosis detection kit (A113-03; Vazyme Biotech Co., Ltd., Nanjing, China). Sections were treated with 100 μL of 20 μg/mL proteinase K solution and incubated at room temperature for 20 min. Next, sections were incubated with 100 μL of 1 × equilibration buffer for 15 min at room temperature. The equilibration buffer was washed off and replaced with terminal deoxynucleotidyl transferase incubation buffer. The sections were placed in a humid incubation chamber and incubated at 37 °C for 60 min. After the sections had been washed with PBS three times, they were stained with DAPI in the dark for 5 min. Finally, the sections were sealed with an anti-fluorescence quenching solution (0100-01; SouthernBiotech, Birmingham, AL, USA) and visualized under a fluorescence microscope.

2.17. Immunohistochemistry (IHC)

Five-micrometer tissue sections were dewaxed in xylene solution (10023418; Sinopharm, Shanghai, China) and rehydrated in a graded ethanol series (10009218; Sinopharm). Antigen retrieval was performed in an autoclave for 5 min, followed by incubation for 20 min with 3 % hydrogen peroxide (H112515; Aladdin, Shanghai, China) to block endogenous peroxidase activity. Then, diluted primary antibodies against Ki67 (1:200; ab16667; Abcam) were added and incubated overnight in a humid incubation chamber at 4 °C. After sections were washed with PBS, they were incubated with secondary antibody (1:200; goat anti-rabbit IgG [H + L] HRP, S0001; Affinity) at 37 °C for 30 min. Subsequently, sections were stained using a liquid diaminobenzidine substrate (BL732A; Biosharp, Hefei, China) and examined under a microscope. Positively stained cells exhibited a brownish color. Harris Hefei (BL702B; Biosharp) was subjected to re-dyeing and sealing with neutral gum (10004160; Sinopharm) before examination under a microscope.

2.18. Statistical analysis

Data analysis was performed using GraphPad Prism Software 9.0 (GraphPad Software, San Diego, CA, USA). Data are presented as means ± standard deviations. Pairwise comparisons between groups were conducted using the least significant difference method in one-way analysis of variance, with statistical significance set at $P < 0.05$. In figures, $P < 0.05$ is indicated by *, whereas $P < 0.01$ is indicated by **.

3. Results

3.1. The hypoxic condition enhanced growth, migration, and GLUT1 expression in ACC cells

Compared with cells cultured under normal conditions, SACC83 and SACC-LM cells under hypoxia exhibited significant increases in viability, proliferation, migration, and invasion ($p < 0.01$), whereas they exhibited a decrease in apoptosis ($p < 0.01$) (Fig. 1A–E). Furthermore, western blotting analysis revealed a significant increase in GLUT1 expression in SACC83 and SACC-LM cells under hypoxic conditions ($p < 0.01$) (Fig. 1F). Immunofluorescence assays were performed to detect the distributions of GLUT1 and the F-actin marker phalloidin in SACC83 and SACC-LM cells. The results showed that hypoxic conditions significantly increased the fluorescence intensity of GLUT1 and its distribution on the cell membranes of SACC83 and SACC-LM cells, compared with cells under

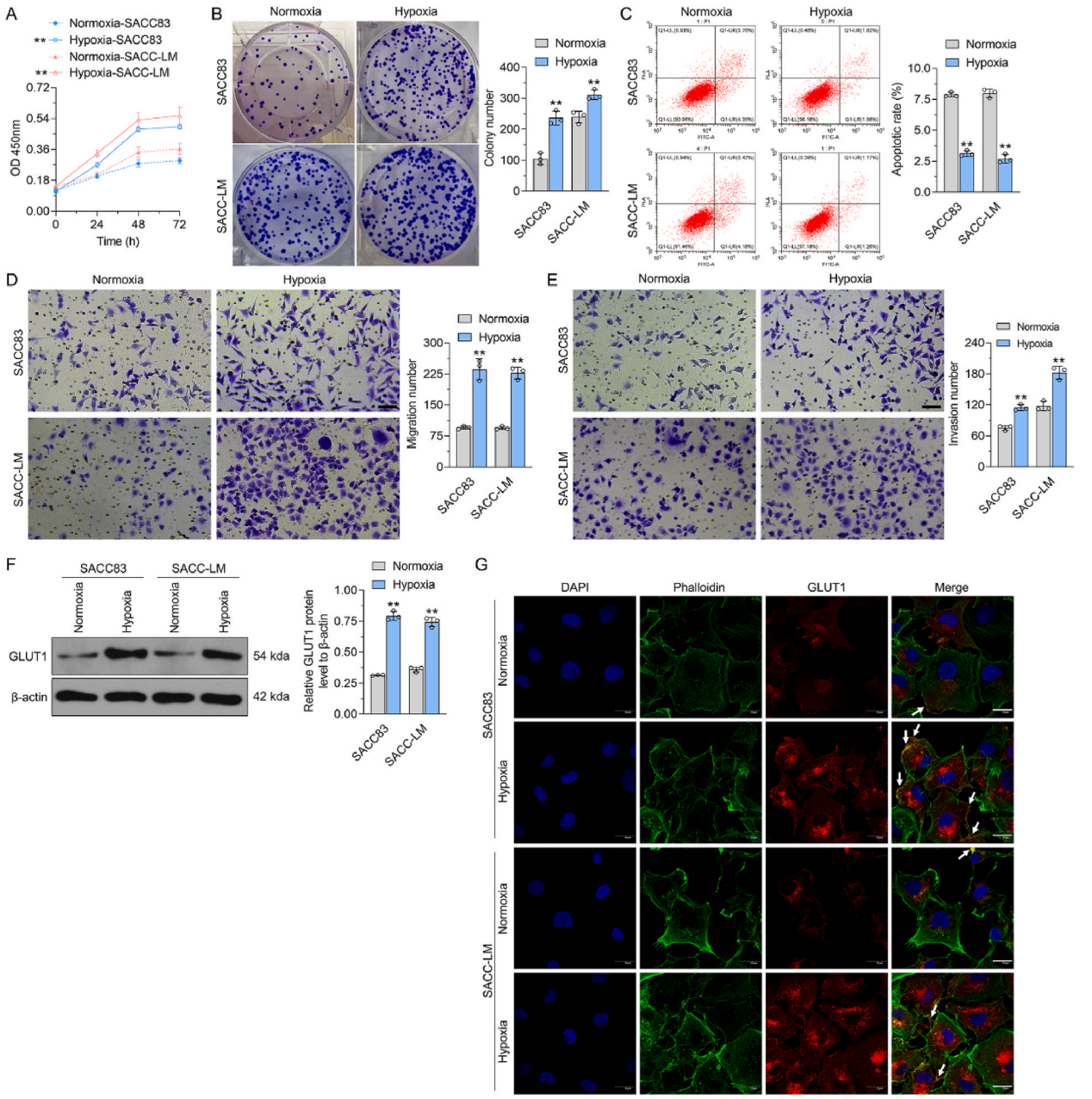

Fig. 1. The Hypoxic condition enhanced growth, migration, and GLUT1 expression in ACC cells. A. viability, B. proliferation, C. migration, D. invasion, E. apoptosis, F. western blotting analysis of GLUT1 expression in SACC83 and SACC-LM cells under hypoxic conditions, G. The fluorescence intensity and distribution of GLUT1 on the cell membranes of SACC83 and SACC-LM cells. Scale bar = 50 μm, **P < 0.01.

normal conditions ($p < 0.01$) (Fig. 1G). These findings suggested that hypoxic conditions enhance growth and metastasis abilities in ACC cells *in vitro*, while upregulating the expression of GLUT1.

3.2. GLUT1 siRNA inhibited growth, migration, and glycolysis in ACC cells under hypoxic condition

Western blotting analysis demonstrated that treatment with GLUT1 siRNA significantly inhibited GLUT1 expression in SACC83 and SACC-LM cells under hypoxic conditions ($p < 0.01$, Fig. 2A). The glycolytic activities of ACC cells treated with NC siRNA or GLUT1 siRNA under hypoxic conditions were then assessed using 2-NBDG and a lactic acid kit. The results showed that GLUT1 siRNA treatment significantly inhibited the hypoxia-induced increases in glucose uptake ($p < 0.01$, Fig. 2B) and lactic acid secretion ($p < 0.01$, Fig. 2C) in SACC83 and SACC-LM cells. Furthermore, treatment with GLUT1 siRNA resulted in decreased cell viability ($p < 0.01$, Fig. 2D), reduced colony formation ($p < 0.01$, Fig. 2E), and increased apoptosis ($p < 0.01$, Fig. 2F) in SACC83 and SACC-LM cells under hypoxic conditions. Moreover, GLUT1 siRNA inhibited the hypoxia-induced promotion of migration ($p < 0.01$, Fig. 2G) and invasion ($p < 0.01$, Fig. 2H) in SACC83 and SACC-LM cells.

3.3. GLUT1 siRNA inhibited autophagy in ACC cells under hypoxic condition

Compared with SACC83 and SACC-LM cells under normal conditions, the ratio of LC3II/LCI was significantly higher in SACC83 and SACC-LM cells under hypoxic conditions ($p < 0.01$, Fig. 3A), whereas p62 expression was significantly reduced ($p < 0.01$, Fig. 3A). These observations indicate that hypoxia can promote autophagy in SACC83 and SACC-LM cells. Furthermore, GLUT1 siRNA led to a significant reduction in the ratio of LC3II/LCI ($p < 0.01$, Fig. 3A) and an increase in p62 expression ($p < 0.01$, Fig. 3A) in SACC83 and SACC-LM cells. Confocal fluorescence microscopy revealed that the numbers of LC3 puncta aggregates in SACC83 and SACC-LM cells were significantly higher under hypoxia than under normal conditions ($p < 0.01$, Fig. 3B), suggesting that hypoxia can stimulate autophagosome formation in SACC83 and SACC-LM cells. GLUT1 siRNA significantly decreased the numbers of LC3 puncta aggregates in SACC83 and SACC-LM cells under hypoxia ($p < 0.01$, Fig. 3B), indicating that GLUT1 siRNA can inhibit the hypoxia-induced promotion of autophagy in SACC83 and SACC-LM cells.

3.4. Combination of GLUT1 siRNA and autophagy inhibitor CQ inhibited proliferation and migration in ACC cells

Compared with cells cultured under normoxia, SACC83 and SACC-LM cells under hypoxia exhibited significant increases in viability, proliferation, migration, and invasion, whereas they exhibited a decrease in apoptosis ($p < 0.01$, Fig. 4A–F). Compared with NC siRNA-treated SACC83 and SACC-LM cells, cells treated with GLUT1 siRNA or CQ alone exhibited significant inhibition of viability, autophagy, cell clones, migration, and invasion under hypoxia ($p < 0.01$, Fig. 4), whereas they showed significant enhancement of

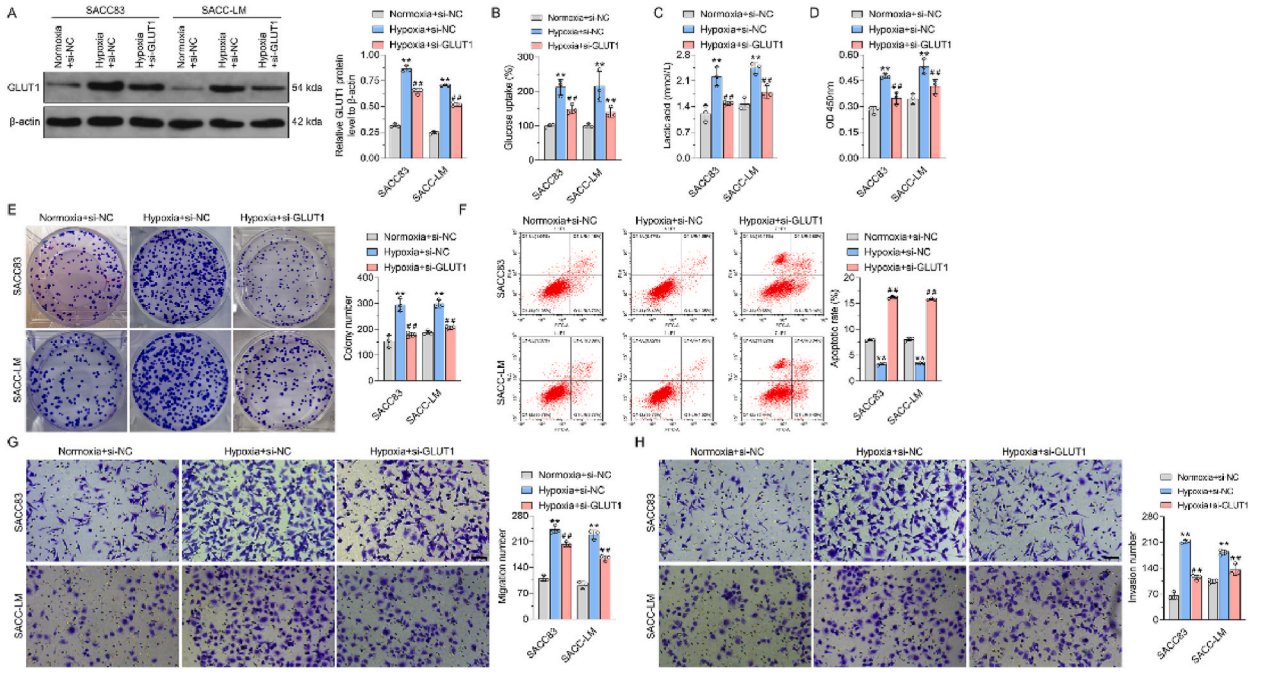

Fig. 2. GLUT1 siRNA inhibited growth, migration, and glycolysis in ACC cells under hypoxic condition. GLUT-1 expression(A), Glucose uptake(B), Lactic acid secretion(C), Cell viability(D), colony formation(E), apoptosis(F), migration(G), and invasion(H) in SACC83 and SACC-LM cells treated by GLUT1 siRNA under hypoxic conditions. Scale bar = 50 μm,**$P < 0.01$, $^{\#\#}P < 0.01$.

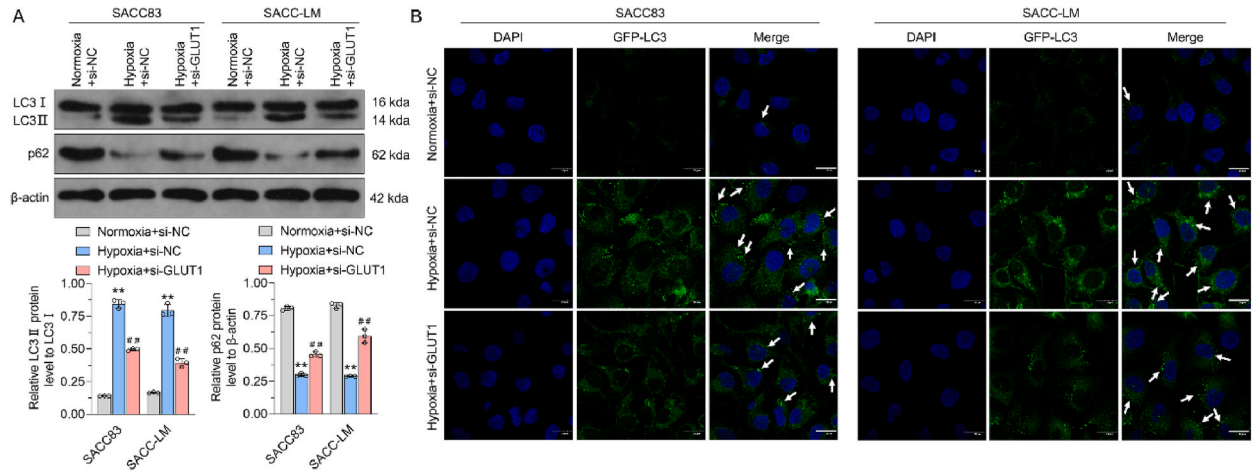

Fig. 3. GLUT1 siRNA inhibited autophagy in ACC cells under hypoxic condition. A. The ratio of LC3II/LCI and p62 expression in SACC83 and SACC-LM cells under hypoxic conditions and treated by GLUT1 siRNA. B. The numbers of LC3 puncta aggregates in SACC83 and SACC-LM cells under hypoxia and treated by GLUT1 siRNA. Scale bar = 50 μm,**P < 0.01, ##P < 0.01.

apoptosis ($p < 0.01$, Fig. 4). Additionally, compared with the effects of GLUT1 siRNA or CQ alone on SACC83 and SACC-LM cells under hypoxia, the combination of GLUT1 siRNA and CQ significantly inhibited proliferation, autophagy, clone formation, migration, and invasion in SACC83 and SACC-LM cells under hypoxia ($p < 0.01$, Fig. 4), whereas it significantly increased apoptosis ($p < 0.01$, Fig. 4). These findings suggest that hypoxia promotes growth and metastasis in ACC cells through GLUT1-mediated autophagy; moreover, the combination of GLUT1 siRNA and CQ has the most potent inhibitory effect on growth and metastasis in ACC cells under hypoxic conditions.

3.5. *Combination of GLUT1 shRNA and autophagy inhibitor CQ inhibited growth and autophagy in vivo*

To investigate the combined effects of inhibiting GLUT1 expression and CQ on the growth of ACC cells *in vivo*, we established a xenograft mouse model with the ACC cell lines SACC83 and SACC-LM. As shown in Fig. 5A, the lentivirus GLUT1 shRNA combined with CQ exhibited a potent inhibitory effect on the growth of ACC cells *in vivo*. Furthermore, none of the treatments affected body weight among mice injected with SACC83 or SACC-LM cells ($p > 0.05$, Fig. 5A), indicating that lentivirus GLUT1 shRNA, CQ alone, and the combination had no apparent toxic side effects in the xenograft mouse model. Histological examination revealed that SACC83 and SACC-LM cells exposed to the combination of GLUT1 shRNA and CQ exhibited the largest area of necrosis and significantly decreased cell density (Fig. 5B). TUNEL staining demonstrated that GLUT1 shRNA, CQ alone, and the combination significantly increased the number of apoptotic cells ($p < 0.01$, Fig. 5C). The numbers of apoptotic SACC83 and SACC-LM cells were highest in mice that received the combination of GLUT1 shRNA and CQ ($p < 0.01$, Fig. 5C). Additionally, IHC analysis indicated that the combination of GLUT1 shRNA and CQ significantly inhibited the expression of Ki67 ($p < 0.01$, Fig. 5D), thus demonstrating that lentivirus GLUT1 shRNA combined with CQ can hinder the growth of xenograft tumors of SACC83 and SACC-LM cells by increasing tumor cell necrosis and apoptosis, while inhibiting Ki67 expression.

To further investigate the effects of GLUT1 expression and autophagy on the growth of ACC cells in xenograft tumors, we examined the expression patterns of GLUT1, LC3II, LC3I, and p62 by western blotting. Lentivirus GLUT1 shRNA significantly inhibited GLUT1 expression in tumor tissues ($p < 0.01$, Fig. 5E). However, CQ did not affect the expression of GLUT1 ($p > 0.05$, Fig. 5E); the inhibitory effect of the combination of GLUT1 shRNA and CQ on the expression of GLUT1 did not significantly differ from the effect of GLUT1 shRNA alone ($p > 0.05$, Fig. 5E). GLUT1 shRNA decreased the LC3II/LCI ratio and increased the expression of p62 in tumor tissues ($p < 0.01$, Fig. 5F), whereas CQ increased the LC3II/LCI ratio and the expression of p62 ($p < 0.01$, Fig. 5F). Therefore, GLUT1 shRNA inhibited autophagy by reducing the expression of GLUT1, whereas CQ inhibited autophagy by blocking autophagic flux. The combination of GLUT1 shRNA and CQ increased the inhibitory effect on autophagy ($p < 0.01$, Fig. 5F). These findings suggest that the inhibition of GLUT1 expression can suppress the growth of xenograft tumors of SACC83 and SACC-LM cells by inhibiting autophagy.

4. Discussion

The high energy demands of cancer cells often result in a hypoxic microenvironment. GLUT1 plays an essential role in the Warburg effect. Its expression is upregulated in human cancers under hypoxic conditions, contributing to proliferation, progression, recurrence, metastasis, chemo-radio resistance, and poor prognosis[13,15–22]. Previous studies have revealed conflicting results regarding the importance of GLUT1 expression in ACC [8,22,23,35]. Costa et al. [8] reported that IHC detected low expression of GLUT1 (40.0 %) in 20 ACCs; they suggested that hypoxia plays a vital role in the high-grade transformation of ACC. In contrast, our previous study showed that 38.1 % of ACCs had GLUT1 expression, which was correlated with ACC recurrence [22]. Additionally, de Souza et al. [35] used

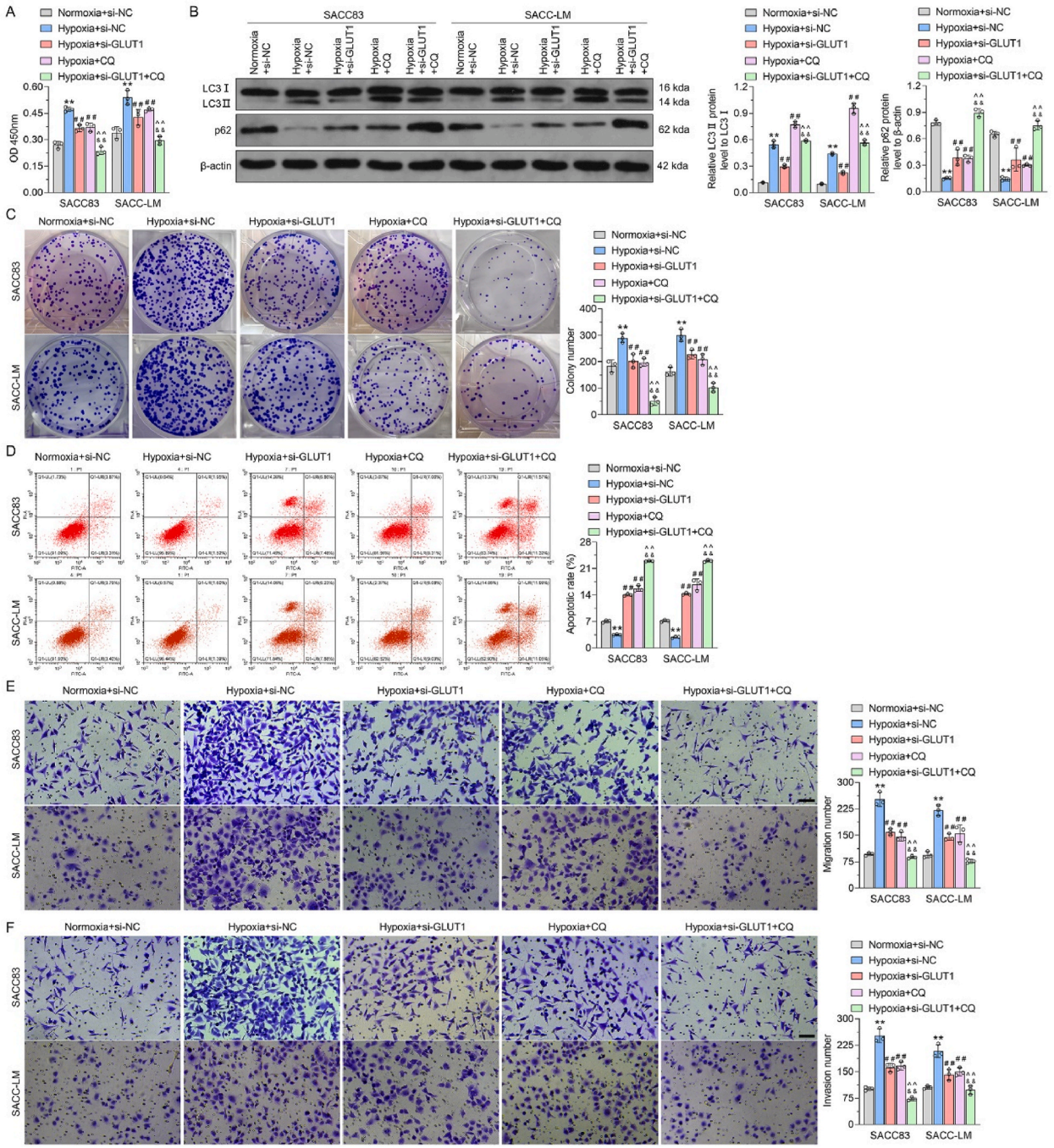

Fig. 4. Combination of GLUT1 siRNA and autophagy inhibitor chloroquine (CQ) inhibited proliferation and migration in ACC cells. Viability (A), autophagy (B), proliferation (C), apoptosis (D),migration, (E), and invasion(F) under hypoxia and treated by GLUT1 siRNA combined with CQ. Scale bar = 50 μm,**P < 0.01, ##P < 0.01.

IHC to examined GLUT1 expression and the angiogenic index in 20 ACCs, 10 mucoepidermoid carcinomas, and 20 pleomorphic adenomas. They detected GLUT1 expression in 90 % of ACCs and found that it was associated with differences in tumor biological behavior [35]. These conflicting findings may be related to the small number of cases and the absence of information concerning ACC etiology and pathogenesis. Our previous study showed that the inhibition of GLUT1 can increase apoptosis and decrease ACC proliferation, suggesting that GLUT1 promotes ACC cell proliferation [23]. The present study revealed that the upregulation of GLUT1 expression under hypoxia was associated with increased proliferation, migration, and invasion and decreased apoptosis in two ACC cell lines, SACC83 and SACC-LM. Furthermore, GLUT1 inhibition can suppress the growth of ACC cells *in vitro* and *in vivo*.

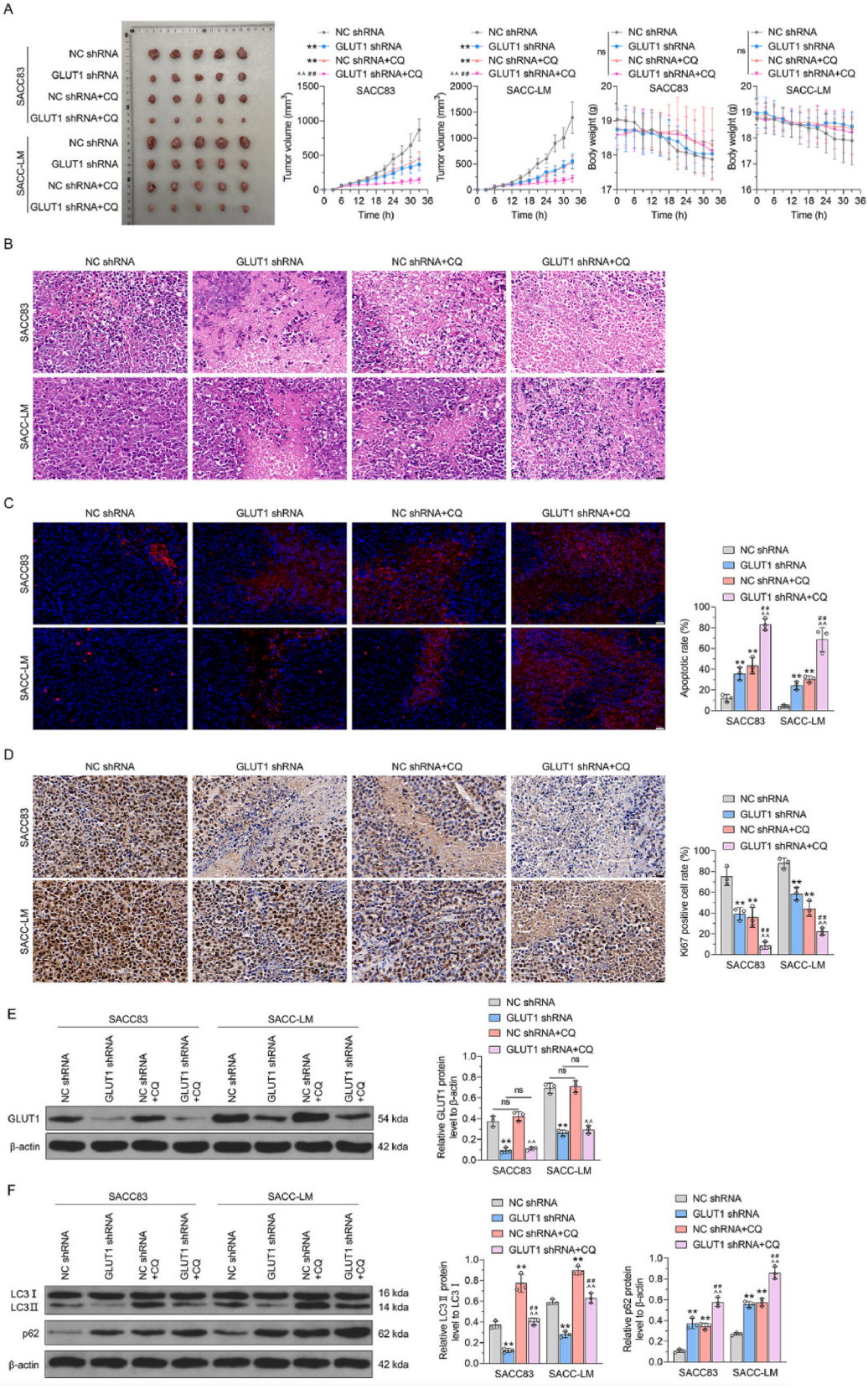

(caption on next page)

Fig. 5. Combination of GLUT1 shRNA and autophagy inhibitor CQ inhibited growth and autophagy *in vivo*. The weight (A), histological examination (B), apoptotic cells(C), Ki67 expression (D), GLUT-1 expression (E), and LC3II/LCI ratio and p62 expression in tumor tissues treated by GLUT1 siRNA combined with CQ *in vivo*. Scale bar = 50 μm,**P < 0.01, ##P < 0.01.

Next, we investigated the mechanisms how GLUT1 contributes to growth, migration, and invasion in ACC cells. Our previous study revealed that hypoxic conditions promote glucose uptake in laryngeal carcinoma cells through the upregulation of GLUT1, leading to increased cell viability and radioresistance [36]. In this study, we observed that glucose uptake and lactic acid secretion increased in SACC83 and SACC-LM cells under hypoxic conditions. However, treatment with GLUT1 siRNA inhibited these effects. These results suggest that GLUT1-mediated glycolysis plays a crucial role in the growth, migration, and invasion of ACC cells under hypoxic conditions. These findings warrant further investigation.

Autophagy has been implicated in cancer growth, invasion, and resistance to treatment[37–39]. Hypoxia can activate autophagy in cancer cells, leading to tumor development[40–42]. Our previous studies demonstrated that autophagy is associated with radioresistance in laryngeal carcinoma [10,26]. Wu et al. [6] reported a significant increase in autophagosome formation and autophagy-related proteins in the ACC-M cell line under hypoxic conditions. Their findings also suggested that autophagy inhibition can reduce invasion by ACC cells. Similarly, Liu et al. [7] observed significant upregulation of autophagy in SACC-LM cells under hypoxia. In the present study, we observed that hypoxia increased the ratio of LC3II/LCI, while decreasing p62 expression, in SACC83 and SACC-LM cells. Autophagy inhibition by CQ inhibited proliferation, migration, and invasion in SACC83 and SACC-LM cells under hypoxia *in vitro*; it also reduced mouse tumor volumes *in vivo*. Furthermore, it has been reported that the inhibition of GLUT1 expression can block autophagy in nucleus pulposus-derived stem cells under hypoxic conditions [43]; GLUT1 knockdown significantly decreased the enhancement of autophagy flux in tamoxifen-resistant breast cancers [44]. Our previous research also showed that the inhibition of GLUT1 expression could suppress autophagy in $CD133^{+}$ laryngeal carcinoma cells under hypoxia and low glucose conditions [19]. In the present study, we found that GLUT1 inhibition suppressed autophagy in SACC83 and SACC-LM cells under hypoxic conditions *in vitro* and in tumor tissues of mice injected with these cells. These findings suggest that GLUT1-mediated autophagy plays a significant role in the growth, migration, and invasion of ACC cells under hypoxic conditions.

Previous studies have revealed that GLUT1 regulates autophagy through an mTORC1-dependent pathway. The mTORC1 pathway plays a central role in the regulation of autophagy, with its inhibition reducing GLUT1 degradation and consequently increasing membrane-localized GLUT1 levels [45]. GLUT1-mediated glucose uptake enhances mTORC1 activation by raising intracellular ATP levels, which are essential for mTORC1 activity [46]. This process decreases the intracellular AMP/ATP ratio, suppresses AMPK activity, promotes protein translation via mTORC1 activation, and ultimately inhibits autophagy.

Our previous studies revealed that the combination of GLUT1 siRNA and curcumin had more potent inhibitory effects on radioresistance in laryngeal carcinoma cells through autophagy regulation, compared with GLUT1 siRNA or curcumin alone [26,47]. In the present study, we investigated the effect of combining GLUT1 siRNA and CQ on proliferation, migration, invasion, and apoptosis in SACC83 and SACC-LM cells under hypoxic conditions *in vitro*. The *in vivo* results were consistent with *in vitro* results. Combined treatment with lentivirus GLUT1 shRNA and CQ significantly inhibited the growth of SACC83 and SACC-LM xenograft tumors by increasing tumor cell necrosis and apoptosis, while inhibiting Ki67 expression, through autophagy inhibition. Therefore, the inhibition of GLUT1 expression, in combination with autophagy inhibition, had the most potent effect on autophagy and the growth of ACC.

5. Conclusion

The findings of this study indicated that GLUT1 promoted growth and migration of ACC cells by regulating autophagy under hypoxic conditions. Furthermore, the combined inhibition of GLUT1 expression and autophagy significantly suppresses the growth of ACC cells both *in vitro* and *in vivo*.

CRediT authorship contribution statement

Kan Liu: Conceptualization, Data curation, Formal analysis, Investigation, Methodology, Writing – original draft. **Jinlong Zhu:** Writing – original draft, Formal analysis, Data curation, Conceptualization. **Yangyang Bao:** Methodology, Formal analysis, Data curation, Conceptualization. **Jin Fang:** Writing – review & editing, Writing – original draft, Supervision, Project administration, Funding acquisition, Conceptualization. **Shuihong Zhou:** Writing – review & editing, Methodology, Formal analysis, Data curation, Conceptualization. **Jun Fan:** Writing – review & editing, Writing – original draft, Methodology, Data curation, Conceptualization.

Data availability

The datasets and analyzed during the current study are available from the corresponding author on reasonable request.

Ethical statement

The institutional review boards of The First Affiliated Hospital, College of Medicine, Zhejiang University, and Zhejiang Sian International Hospital (approval no. 2021-009) approved the study protocol. And all experiments were performed in accordance with relevant guidelines and regulations. All methods are reported in accordance with ARRIVE guidelines. All authors had access to the

study data and approved the final manuscript.

Funding

Health Commission of Zhejiang Province, China (No. 2021KY1128).

Declaration of competing interest

The authors declare that they have no known competing financial interests or personal relationships that could have appeared to influence the work reported in this paper.

Acknowledgements

None.

References

[1] C. Emerick, F.V. Mariano, P.A. Vargas, J.E. Nör, C.H. Squarize, R.M. Castilho, Adenoid Cystic Carcinoma from the salivary and lacrimal glands and the breast: different clinical outcomes to the same tumor, Crit. Rev. Oncol. Hematol. 179 (2022) 103792, https://doi.org/10.1016/j.critrevonc.2022.103792.
[2] S. Cozzi, L. Bardoscia, M. Najafi, A. Botti, G. Blandino, M. Augugliaro, M. Manicone, F. Iori, L. Giaccherini, A. Sardaro, C. Iotti, P. Ciammella, Adenoid cystic carcinoma/basal cell carcinoma of the prostate: overview and update on rare prostate cancer subtypes, Curr. Oncol. 29 (2022) 1866–1876, https://doi.org/10.3390/curroncol29030152.
[3] PRIMARY CUTANEOUS ADENOID CYSTIC CARCINOMA IN THE TRUNK: CASE REPORT AND LITERATURE REVIEW, Exp. Oncol. 44 (2022), https://doi.org/10.32471/exp-oncology.2312-8852.vol-44-no-2.18006.
[4] Y. Fang, Z. Peng, Y. Wang, K. Gao, Y. Liu, R. Fan, H. Zhang, Z. Xie, W. Jiang, Current opinions on diagnosis and treatment of adenoid cystic carcinoma, Oral Oncol. 130 (2022) 105945, https://doi.org/10.1016/j.oraloncology.2022.105945.
[5] Z. Chen, H. Wu, S. Huang, W. Li, S. Zhang, P. Zheng, X. Zhou, W. Liu, D. Zhang, Expression of BNIP3 and its correlations to hypoxia-induced autophagy and clinicopathological features in salivary adenoid cystic carcinoma, Cancer Biomarkers 15 (2015) 467–475, https://doi.org/10.3233/CBM-150474.
[6] H. Wu, S. Huang, Z. Chen, W. Liu, X. Zhou, D. Zhang, Hypoxia-induced autophagy contributes to the invasion of salivary adenoid cystic carcinoma through the HIF-1α/BNIP3 signaling pathway, Mol. Med. Rep. 12 (2015) 6467–6474, https://doi.org/10.3892/mmr.2015.4255.
[7] C. Liu, S. Li, F. Pang, H. Wu, L. Chai, C. Liang, D. Zhang, Autophagy-related gene expression regulated by HIF-1α in salivary adenoid cystic carcinoma, Oral Dis. 25 (2019) 1076–1083, https://doi.org/10.1111/odi.13058.
[8] A.F. Costa, M.G. Tasso, F.V. Mariano, A.B. Soares, C.T. Chone, A.N. Crespo, M.F. Fresno, J.L. Llorente, C. Suárez, V.C. De Araújo, M. Hermsen, A. Altemani, Levels and patterns of expression of hypoxia-inducible factor-1α, vascular endothelial growth factor, glucose transporter-1 and CD105 in adenoid cystic carcinomas with high-grade transformation: hypoxia in adenoid cystic carcinoma, Histopathology 60 (2012) 816–825, https://doi.org/10.1111/j.1365-2559.2011.04128.x.
[9] J.-T. Zhong, S.-H. Zhou, Warburg effect, hexokinase-II, and radioresistance of laryngeal carcinoma, Oncotarget 8 (2017) 14133–14146, https://doi.org/10.18632/oncotarget.13044.
[10] X.-H. Chen, D.-L. Yu, J.-T. Zhong, S.-H. Zhou, J. Fan, Z.-J. Lu, Targeted inhibition of HK-II reversed the Warburg effect to improve the radiosensitivity of laryngeal carcinoma, Cancer Manag. Res. 13 (2021) 8063–8076, https://doi.org/10.2147/CMAR.S324754.
[11] H. Yang, J.-T. Zhong, S.-H. Zhou, H.-M. Han, Roles of GLUT-1 and HK-II expression in the biological behavior of head and neck cancer, Oncotarget 10 (2019) 3066–3083, https://doi.org/10.18632/oncotarget.24684.
[12] X.-H. Chen, Y.-Y. Bao, S.-H. Zhou, Q.-Y. Wang, Y. Wei, J. Fan, Glucose transporter-1 expression in CD133+ laryngeal carcinoma Hep-2 cells, Mol. Med. Rep. 8 (2013) 1695–1700, https://doi.org/10.3892/mmr.2013.1740.
[13] Y.-J. Ao, S.-H. Zhou, Primary poorly differentiated small cell type neuroendocrine carcinoma of the hypopharynx, OncoTargets Ther. 12 (2019) 1593–1601, https://doi.org/10.2147/OTT.S189241.
[14] Y.-J. Ao, T.-T. Wu, Z.-Z. Cao, S.-H. Zhou, Y.-Y. Bao, L.-F. Shen, Role and mechanism of Glut-1 and H+/K+-ATPase expression in pepsin-induced development of vocal cord leukoplakia, Eur. Arch. Otorhinolaryngol. 279 (2022) 1413–1424, https://doi.org/10.1007/s00405-021-07172-y.
[15] Y.-Y. Bao, S.-H. Zhou, Z.-J. Lu, J. Fan, Y.-P. Huang, Inhibiting GLUT-1 expression and PI3K/Akt signaling using apigenin improves the radiosensitivity of laryngeal carcinoma in vivo, Oncol. Rep. 34 (2015) 1805–1814, https://doi.org/10.3892/or.2015.4158.
[16] Y.-Y. Bao, S.-H. Zhou, J. Fan, Q.-Y. Wang, Anticancer mechanism of apigenin and the implications of *GLUT-1* expression in head and neck cancers, Future Oncol. 9 (2013) 1353–1364, https://doi.org/10.2217/fon.13.84.
[17] J. Fang, S.-H. Zhou, J. Fan, S.-X. Yan, Roles of glucose transporter-1 and the phosphatidylinositol 3-kinase/protein kinase B pathway in cancer radioresistance, Mol. Med. Rep. 11 (2015) 1573–1581, https://doi.org/10.3892/mmr.2014.2888 (Review).
[18] X.-H. Wu, S.-P. Chen, J.-Y. Mao, X.-X. Ji, H.-T. Yao, S.-H. Zhou, Expression and significance of hypoxia-inducible factor-1α and glucose transporter-1 in laryngeal carcinoma, Oncol. Lett. 5 (2013) 261–266, https://doi.org/10.3892/ol.2012.941.
[19] X.-H. Chen, J. Liu, J.-T. Zhong, S.-H. Zhou, J. Fan, Effect of GLUT1 inhibition and autophagy modulation on the growth and migration of laryngeal carcinoma stem cells under hypoxic and low-glucose conditions, OncoTargets Ther. 14 (2021) 3069–3081, https://doi.org/10.2147/OTT.S300423.
[20] X.-M. Luo, S.-H. Zhou, J. Fan, Glucose transporter-1 as a new therapeutic target in laryngeal carcinoma, J. Int. Med. Res. 38 (2010) 1885–1892, https://doi.org/10.1177/147323001003800601.
[21] Y. Li, L. Zhao, Y. Huo, X. Yang, Y. Li, H. Xu, X.-F. Li, Visualization of hypoxia in cancer cells from effusions in animals and cancer patients, Front. Oncol. 12 (2022) 1019360, https://doi.org/10.3389/fonc.2022.1019360.
[22] J. Fang, Y.-Y. Bao, S.-H. Zhou, X.-M. Luo, H.-T. Yao, J.-F. He, Q.-Y. Wang, Recurrent prognostic factors and expression of GLUT-1, PI3K and p-Akt in adenoid cystic carcinomas of the head and neck: clinicopathological features and biomarkers of adenoid cystic carcinoma, Oncol. Lett. 4 (2012) 1234–1240, https://doi.org/10.3892/ol.2012.895.
[23] J. Fang, Y.-Y. Bao, S.-H. Zhou, J. Fan, Apigenin inhibits the proliferation of adenoid cystic carcinoma via suppression of glucose transporter-1, Mol. Med. Rep. 12 (2015) 6461–6466, https://doi.org/10.3892/mmr.2015.4233.
[24] S.T. Bradley, Y. Lee, Z. Gurel, R.J. Kimple, Autophagy awakens—the myriad roles of autophagy in head and neck cancer development and therapeutic response, Mol. Carcinog. 61 (2022) 243–253, https://doi.org/10.1002/mc.23372.
[25] Y.-J. Hu, J.-T. Zhong, L. Gong, S.-C. Zhang, S.-H. Zhou, Autophagy-related beclin 1 and head and neck cancers, OncoTargets Ther. 13 (2020) 6213–6227, https://doi.org/10.2147/OTT.S256072.
[26] L. Dai, Q. Yu, S. Zhou, Y. Bao, J. Zhong, L. Shen, Z. Lu, J. Fan, Y. Huang, Effect of combination of curcumin and GLUT -1 AS-ODN on radiosensitivity of laryngeal carcinoma through regulating autophagy, HEAD NECK-J. Sci. Spec. HEAD NECK 42 (2020) 2287–2297, https://doi.org/10.1002/hed.26180.

[27] J. Gao, K. Ma, L. Zhang, T. Li, B. Zhao, Y. Jiang, Paired related homeobox 1 attenuates autophagy via acetyl-CoA carboxylase 1-regulated fatty acid metabolism in salivary adenoid cystic carcinoma, FEBS Open Bio 12 (2022) 1006–1016, https://doi.org/10.1002/2211-5463.13367.
[28] L. Liang, J. Weng, Y. You, Q. He, Y. Fan, G. Liao, Role of Noxa in proliferation, apoptosis, and autophagy in human adenoid cystic carcinoma, J. Oral Pathol. Med. 48 (2019) 52–59, https://doi.org/10.1111/jop.12787.
[29] X.-Y. Ge, L.-Q. Yang, Y. Jiang, W.-W. Yang, J. Fu, S.-L. Li, Reactive oxygen species and autophagy associated apoptosis and limitation of clonogenic survival induced by zoledronic acid in salivary adenoid cystic carcinoma cell line SACC-83, PLoS One 9 (2014) e101207, https://doi.org/10.1371/journal.pone.0101207.
[30] C. Jiang, S. Jin, Z. Jiang, J. Wang, Inhibitory effects of silibinin on proliferation and lung metastasis of human high metastasis cell line of salivary gland adenoid cystic carcinoma via autophagy induction, OncoTargets Ther. 9 (2016) 6609–6618, https://doi.org/10.2147/OTT.S107101.
[31] J.A.V. Goulart-Filho, V.A.M. Montalli, F. Passador-Santos, N.S. De Araújo, V.C. De Araújo, Role of apoptotic, autophagic and senescence pathways in minor salivary gland adenoid cystic carcinoma, Diagn. Pathol. 14 (2019) 14, https://doi.org/10.1186/s13000-019-0796-2.
[32] M. Nishida, N. Yamashita, T. Ogawa, K. Koseki, E. Warabi, T. Ohue, M. Komatsu, H. Matsushita, K. Kakimi, E. Kawakami, K. Shiroguchi, H. Udono, Mitochondrial reactive oxygen species trigger metformin-dependent antitumor immunity via activation of Nrf2/mTORC1/p62 axis in tumor-infiltrating CD8T lymphocytes, J. Immunother. Cancer 9 (2021) e002954, https://doi.org/10.1136/jitc-2021-002954.
[33] M. Fu, Q. Gao, M. Xiao, X.-Y. Sun, S.-L. Li, X.-Y. Ge, NAT10/CEBPB/vimentin signalling axis promotes adenoid cystic carcinoma malignant phenotypes in vitro, Oral Dis. 30 (2024) 4341–4355, https://doi.org/10.1111/odi.14879.
[34] J. Boizot, M. Minville-Walz, D.P. Reinhardt, M. Bouschbacher, P. Sommer, D. Sigaudo-Roussel, R. Debret, FBN2 silencing recapitulates hypoxic conditions and induces elastic fiber impairment in human dermal fibroblasts, Int. J. Mol. Sci. 23 (2022) 1824, https://doi.org/10.3390/ijms23031824.
[35] L.B. De Souza, L.C. De Oliveira, C.F.W. Nonaka, M.L.D.D.S. Lopes, L.P. Pinto, L.M.G. Queiroz, Immunoexpression of GLUT-1 and angiogenic index in pleomorphic adenomas, adenoid cystic carcinomas, and mucoepidermoid carcinomas of the salivary glands, Eur. Arch. Otorhinolaryngol. 274 (2017) 2549–2556, https://doi.org/10.1007/s00405-017-4530-y.
[36] Y. Bao, J. Zhong, L. Shen, L. Dai, S. Zhou, J. Fan, H. Yao, Z. Lu, Effect of Glut-1 and HIF-1α double knockout by CRISPR/CAS9 on radiosensitivity in laryngeal carcinoma via the PI3K/Akt/mTOR pathway, J. Cell Mol. Med. 26 (2022) 2881–2894, https://doi.org/10.1111/jcmm.17303.
[37] W. Yang, B. Cheng, P. Chen, X. Sun, Z. Wen, Y. Cheng, BTN3A1 promotes tumor progression and radiation resistance in esophageal squamous cell carcinoma by regulating ULK1-mediated autophagy, Cell Death Dis. 13 (2022) 984, https://doi.org/10.1038/s41419-022-05429-w.
[38] Y. Xue, X. Jiang, J. Wang, Y. Zong, Z. Yuan, S. Miao, X. Mao, Effect of regulatory cell death on the occurrence and development of head and neck squamous cell carcinoma, Biomark. Res. 11 (2023) 2, https://doi.org/10.1186/s40364-022-00433-w.
[39] X. Yan, X. Qu, B. Liu, Y. Zhao, L. Xu, S. Yu, J. Wang, L. Wang, J. Su, Autophagy-induced HDAC6 activity during hypoxia regulates mitochondrial energy metabolism through the β-catenin/COUP-TFII Axis in hepatocellular carcinoma cells, Front. Oncol. 11 (2021) 742460, https://doi.org/10.3389/fonc.2021.742460.
[40] A.A.A.Y. AlMuzaini, K. Boesze-Battaglia, F. Alawi, S.O. Akintoye, Hypoxia enhances basal autophagy of epithelial-derived ameloblastoma cells, Oral Dis. 28 (2022) 2175–2184, https://doi.org/10.1111/odi.13848.
[41] E. Mahgoub, J. Taneera, N. Sulaiman, M. Saber-Ayad, The role of autophagy in colorectal cancer: impact on pathogenesis and implications in therapy, Front. Med. 9 (2022) 959348, https://doi.org/10.3389/fmed.2022.959348.
[42] G. Chen, Y. Zhang, J. Liang, W. Li, Y. Zhu, M. Zhang, C. Wang, J. Hou, Deregulation of hexokinase II is associated with glycolysis, autophagy, and the epithelial-mesenchymal transition in tongue squamous cell carcinoma under hypoxia, BioMed Res. Int. 2018 (2018) 1–15, https://doi.org/10.1155/2018/8480762.
[43] R. He, Z. Wang, M. Cui, S. Liu, W. Wu, M. Chen, Y. Wu, Y. Qu, H. Lin, S. Chen, B. Wang, Z. Shao, HIF1A Alleviates compression-induced apoptosis of nucleus pulposus derived stem cells via upregulating autophagy, Autophagy 17 (2021) 3338–3360, https://doi.org/10.1080/15548627.2021.1872227.
[44] M. Sun, S. Zhao, Y. Duan, Y. Ma, Y. Wang, H. Ji, Q. Zhang, GLUT1 participates in tamoxifen resistance in breast cancer cells through autophagy regulation, Naunyn-Schmiedebergs Arch Pharmacol 394 (2021) 205–216, https://doi.org/10.1007/s00210-020-01893-3.
[45] D. Zhou, Y. Yao, L. Zong, G. Zhou, M. Feng, J. Chen, G. Liu, G. Chen, K. Sun, H. Yao, Y. Liu, X. Shi, W. Zhang, B. Shi, Q. Tai, G. Wu, L. Sun, W. Hu, X. Zhu, S. He, TBK1 facilitates GLUT1-dependent glucose consumption by suppressing mTORC1 signaling in colorectal cancer progression, Int. J. Biol. Sci. 18 (2022) 3374–3389, https://doi.org/10.7150/ijbs.70742.
[46] L.-B. Dai, J.-T. Zhong, L.-F. Shen, S.-H. Zhou, Z.-J. Lu, Y.-Y. Bao, J. Fan, Radiosensitizing effects of curcumin alone or combined with GLUT1 siRNA on laryngeal carcinoma cells through AMPK pathway-induced autophagy, J. Cell Mol. Med. (2021), https://doi.org/10.1111/jcmm.16450.
[47] L. Dai, J. Zhong, L. Shen, S. Zhou, Z. Lu, Y. Bao, J. Fan, Radiosensitizing effects of curcumin alone or combined with GLUT1 siRNA on laryngeal carcinoma cells through AMPK pathway-induced autophagy, J. Cell Mol. Med. 25 (2021) 6018–6031, https://doi.org/10.1111/jcmm.16450.